Mineralogical Magazine (2019), **83**, 781–790
doi:10.1180/mgm.2019.17

CAMBRIDGE UNIVERSITY PRESS

Article

Antofagastaite, $Na_2Ca(SO_4)_2 \cdot 1.5H_2O$, a new mineral related to syngenite

Igor V. Pekov[1]*, Vadim M. Kovrugin[2,3], Oleg I. Siidra[2,4], Nikita V. Chukanov[5], Dmitry I. Belakovskiy[6], Natalia N. Koshlyakova[1], Vasiliy O. Yapaskurt[1], Anna G. Turchkova[1] and Gerhard Möhn[7]

[1]Faculty of Geology, Moscow State University, Vorobievy Gory, 119991 Moscow, Russia; [2]Department of Crystallography, St Petersburg State University, University Embankment 7/9, 199034 St Petersburg, Russia; [3]Laboratoire de Réactivité et Chimie des Solides, UMR 7314 CNRS, Université de Picardie Jules Verne, 33 rue St Leu, 80039 Amiens, France; [4]Nanomaterials Research Center, Kola Science Center, Russian Academy of Sciences, 184200 Apatity, Russia; [5]Institute of Problems of Chemical Physics, Russian Academy of Sciences, 142432 Chernogolovka, Moscow region, Russia; [6]Fersman Mineralogical Museum of the Russian Academy of Sciences, Leninsky Prospekt 18-2, 119071 Moscow, Russia; and [7]Dr.-J.-Wittemannstrasse 5, 65527 Niedernhausen, Germany

Abstract

The new mineral antofagastaite, ideally $Na_2Ca(SO_4)_2 \cdot 1.5H_2O$, was found in the oxidation zone of sulfide–quartz veins at the abandoned Coronel Manuel Rodríguez mine, Mejillones, Antofagasta Province, Antofagasta Region, Chile. It is associated with sideronatrite, metasideronatrite, aubertite, gypsum, ferrinatrite, glauberite, amarillite and an unidentified Fe phosphate. Antofagastaite occurs as prismatic crystals up to 0.5 mm × 1 mm × 5 mm, elongated along [010], typically combined in open-work aggregates up to 1 cm across. Antofagastaite is transparent and colourless, with vitreous lustre. It is brittle; the Mohs' hardness is *ca* 3. Cleavage is distinct on (001). $D_{meas.}$ is 2.42(1) and $D_{calc.}$ is 2.465 g cm^{-3}. Antofagastaite is optically biaxial (–), $\alpha = 1.489(2)$, $\beta = 1.508(2)$, $\gamma = 1.510(2)$ and $2V_{meas.} = 40(10)°$. The IR spectrum is reported. Chemical composition (wt.%, electron microprobe, H_2O determined by gas chromatography) is: Na_2O 20.85, CaO 17.42, SO_3 52.56, H_2O 7.93, total 98.76. The empirical formula (based on 8 O atoms belonging to sulfate anions per formula unit with all H belonging to H_2O molecules) is $Na_{2.06}Ca_{0.95}S_{2.01}O_8 \cdot 1.35H_2O$. Antofagastaite is monoclinic, $P2_1/m$, $a = 6.4596(4)$, $b = 6.8703(5)$, $c = 9.4685(7)$ Å, $\beta = 104.580(4)°$, $V = 406.67(5)$ Å^3 and $Z = 2$. The strongest reflections of the powder XRD pattern [*d*, Å (*I*, %) (*hkl*)] are: 9.17 (100) (001), 5.501 (57) (011), 3.437 (59) (020), 3.058 (43) (003), 2.918 (50) ($\bar{2}$11), 2.795 (35) (013) and 2.753 (50) (121, 201). The crystal structure was solved based on single-crystal X-ray diffraction data, $R_1 = 5.71\%$. The structure of antofagastaite consists of ordered and disordered blocks and is related to syngenite $K_2Ca(SO_4)_2 \cdot H_2O$. Incorporation of additional H_2O molecules in the syngenite-type structure results in disorder of the one of the two tetrahedral sulfate groups occurring in antofagastaite. In addition to the above-reported type material, antofagastaite together with syngenite and blödite occurs in the Arsenatnaya fumarole, Tolbachik volcano, Kamchatka, Russia.

Keywords: antofagastaite, new mineral, hydrated sodium calcium sulfate, syngenite, crystal structure, oxidation zone of ore deposit, Coronel Manuel Rodríguez mine, Atacama Desert, fumarole, Tolbachik volcano

(Received 19 November 2018; accepted 17 February 2019; Accepted Manuscript published online: 12 April 2019; Associate Editor: František Laufek)

Introduction

The family of hydrated sodium-calcium sulfates with the general formula $Na_xCa_y(SO_4)_{0.5x+y} \cdot nH_2O$ includes a dozen natural and synthetic phases. This family demonstrates a truly enigmatic case: despite chemical simplicity, the majority of these compounds are poorly characterised. Until recently, four valid mineral species belonging to this family were known: wattevilleite, $Na_2Ca(SO_4)_2 \cdot 4H_2O$ (?) (Palache *et al.*, 1951; Sabelli and Trosti-Ferroni, 1985; Leverett and Williams, 2007), hydroglauberite, $Na_{10}Ca_3(SO_4)_8 \cdot 6H_2O$ (Slyusareva, 1969), eugsterite, $Na_4Ca(SO_4)_3 \cdot 2H_2O$ (Vergouwen, 1981), and omongwaite, $Na_2Ca_5(SO_4)_6 \cdot 3H_2O$ (Mees *et al.*, 2008). None of these minerals were studied using a single-crystal diffraction method due to the imperfectness of their crystals. Moreover, unit-cell data are still unknown for wattevilleite, hydroglauberite and eugsterite. Among synthetic hydrated Na–Ca sulfates, the crystal structure has only been solved for $NaCa_3(SO_4)_{3.5} \cdot 1.7H_2O$ which was found to be structurally similar to bassanite $CaSO_4 \cdot 0.5H_2O$ (Freyer *et al.*, 1999). This synthetic Na–Ca sulfate and omongwaite have close powder X-ray diffraction patterns that allowed us to determine unit-cell parameters of the latter and consider its crystal structure as bassanite-related (Mees *et al.*, 2008).

The present paper is devoted to the new mineral species antofagastaite (Cyrillic: антофагастаит), ideally $Na_2Ca(SO_4)_2 \cdot 1.5H_2O$, which belongs to the same chemical family but significantly differs from all its other representatives as well as from known synthetic Na–Ca sulfates. The mineral is named after the Antofagasta Province (Northern Chile) in which its type locality, the Coronel Manuel Rodríguez mine is situated. We note that the similar name 'antofagastite' was proposed in 1938 for a mineral with

***Author for correspondence:** Igor V. Pekov, Email: igorpekov@mail.ru
Cite this article: Pekov I.V., Kovrugin V.M., Siidra O.I., Chukanov N.V., Belakovskiy D.I., Koshlyakova N.N., Yapaskurt V.O., Turchkova A.G. and Möhn G. (2019) Antofagastaite, $Na_2Ca(SO_4)_2 \cdot 1.5H_2O$, a new mineral related to syngenite. *Mineralogical Magazine* **83**, 781–790. https://doi.org/10.1180/mgm.2019.17

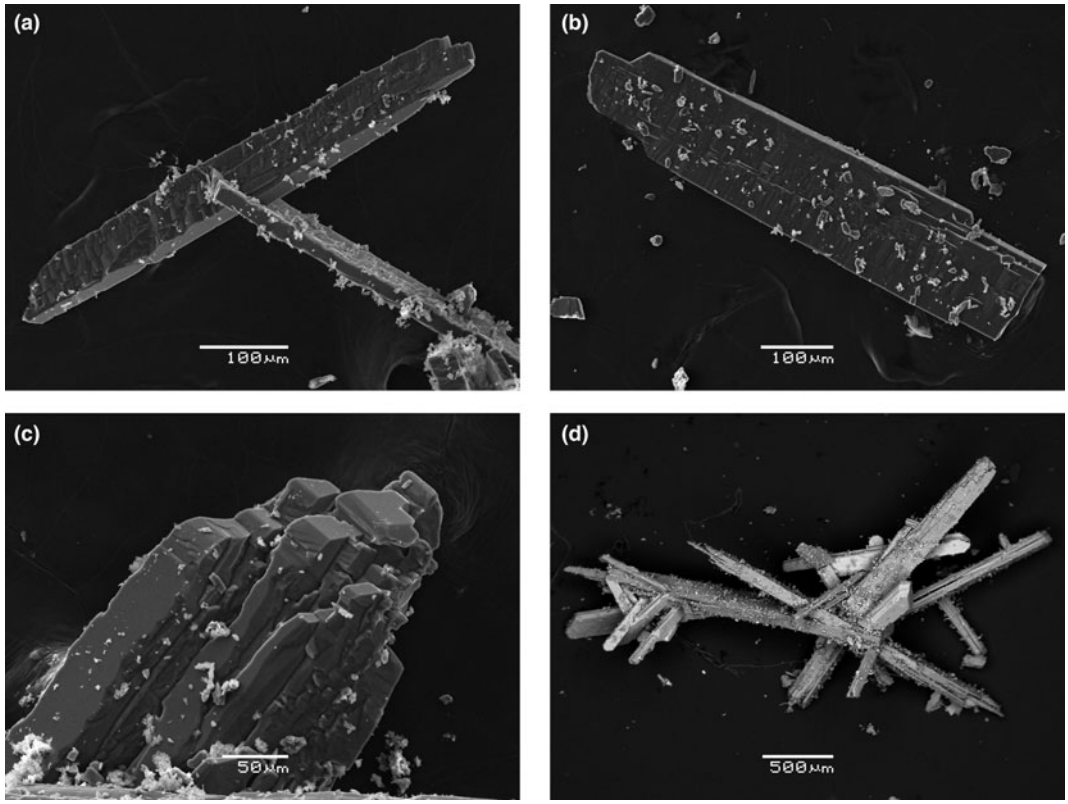

Fig. 1. Morphology of crystals and aggregates of antofagastaite from the Coronel Manuel Rodríguez mine: (*a*) cluster of flattened prismatic crystals; (*b*) board-shaped crystal with overgrowing tiny crystals of an unidentified Fe phosphate; (*c*) parallel intergrowth of prismatic crystals; (*d*) open-work group of slightly divergent prismatic crystals with metasideronatrite crystals (lighter). Scanning electron microscopy (SEM) images: (*a*)-(*c*) – in secondary electron (SE) mode, (*d*) – in back-scattered electron (BSE) mode, specimen no. CMR-5052.

the formula $CuCl_2{\cdot}2H_2O$, considered initially as a new species (Palache and Foshag, 1938). However, it was later shown to be identical to the earlier described eriochalcite and the name 'antofagastite' was therefore discredited (Palache *et al.*, 1951).

Both the new mineral antofagastaite and its name have been approved by the IMA Commission on New Minerals, Nomenclature and Classification (IMA-CNMNC), IMA2018-049. The type specimen is deposited in the collection of the Fersman Mineralogical Museum of the Russian Academy of Sciences, Moscow, with the catalogue number 96263.

After completion of the investigation of antofagastaite from the Coronel Manuel Rodríguez mine (the holotype) and its approval as a new species by the IMA-CNMNC, the same mineral was identified by us in the material from the Arsenatnaya fumarole at the Tolbachik volcano, Kamchatka, Russia, and studied including the crystal structure determination. We consider it of interest to include a brief description of this, the second find of antofagastaite in the present paper.

Occurrence and general appearance

Specimens which became the type material of the new mineral were collected by us in January 2016 in dumps of the abandoned Coronel Manuel Rodríguez copper mine near the city of Antofagasta, Mejillones Peninsula, Mejillones, Antofagasta Province, Antofagasta Region, Chile (Mills *et al.*, 2012).

Antofagastaite from the type locality is a supergene mineral formed in the oxidation zone of sulfide–quartz veins under conditions of extremely arid climate, typical for the Atacama Desert. It occurs in cavernous aggregates mainly composed of sideronatrite (partly altered to metasideronatrite), aubertite and gypsum. Other associated minerals are ferrinatrite, glauberite, amarillite and an unidentified Fe phosphate. Quartz is a relict gangue mineral found in this assemblage.

At the Coronel Manuel Rodríguez mine antofagastaite occurs as prismatic crystals up to 0.5 mm × 1 mm × 5 mm (typically less, up to 1 mm long) elongated along [010] and commonly flattened on [100]. They are usually coarse, sometimes blocky, slightly divergent and spear-like. The major form of antofagastaite crystals is the pinacoid {100} (Figs 1*a* and *b*). The lateral faces were not indexed. Faces of the pinacoid {010} are observed on well-terminated crystals (Fig. 1*c*). Parallel or near-parallel intergrowths of crystals are observed (Fig. 1*c*) as well as chaotic, open-work aggregates up to 1 cm across occurring in cavities. The new mineral overgrows sideronatrite/metasideronatrite and aubertite or forms intimate intergrowths with these hydrous Na–Fe sulfates (Figs 1*d* and 2). Some antofagastaite crystals are sprinkled by tiny tabular crystals of an unidentified Fe phosphate and contain inclusions of glauberite and amarillite (Figs 1*b* and 3).

At the Tolbachik volcano, antofagastaite was found in the Arsenatnaya fumarole located on the summit of the Second scoria cone of the Northern Breakthrough of the Great Tolbachik Fissure Eruption of 1975–1976. The description of this active and richly mineralised fumarole has been given by Pekov *et al.* (2018). Antofagastaite occurs in the upper, moderately hot zone (temperatures measured by us in different areas of this zone are 70–150°C) of the fumarole in which the complex interactions between volcanic gas, atmospheric agents (water, water vapour

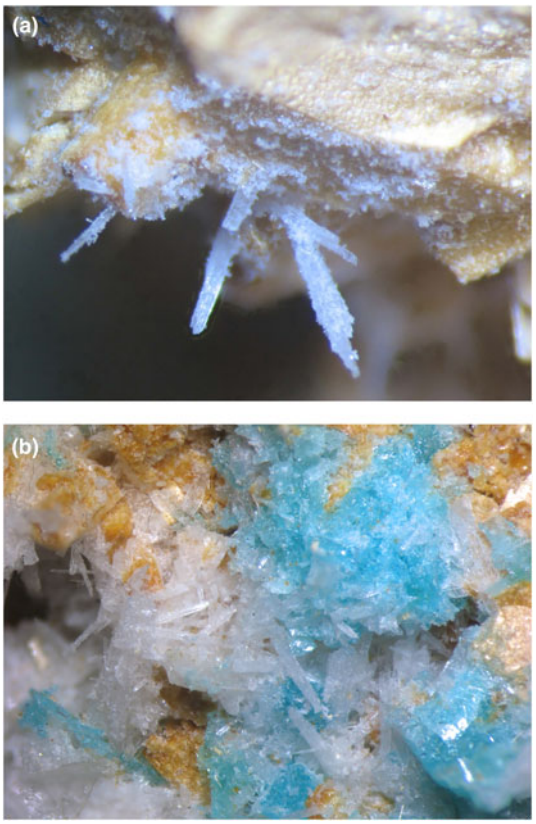

Fig. 2. Colourless prismatic crystals of antofagastaite from the Coronel Manuel Rodríguez mine: (*a*) on yellowish metasideronatrite; (*b*) on orange–yellow sideronatrite (partially altered to metasideronatrite) with blue aubertite. Field of view width: (*a*) 3.8 mm and (*b*) 8.9 mm. Photo: I.V. Pekov and A.V. Kasatkin, specimen no. CMR-5052.

and CO_2) and earlier formed sublimate minerals take place. Antofagastaite forms in cavities long prismatic, lath-shaped to acicular crystals up to 0.03 mm × 0.3 mm associated closely with syngenite (Fig. 4) and blödite. An earlier, high-temperature assemblage of sublimate minerals include: hematite, anhydrite, aphthitalite, fluorophlogopite, sanidine (As-bearing), johillerite, svabite, tilasite and zubkovaite $Ca_3Cu_3(AsO_4)_4$ (IMA2018-008, Pekov et al., 2019).

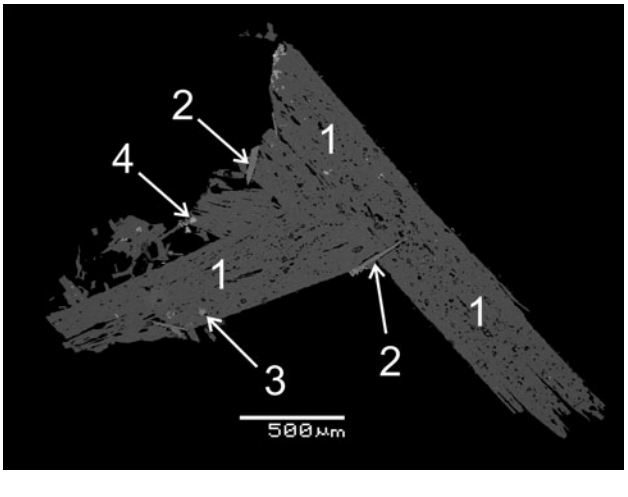

Fig. 3. Polished section of a cluster of antofagastaite crystals (1; porosity is very visible) with glauberite (2), amarillite (3) and an unidentified Fe phosphate (4). Coronel Manuel Rodríguez mine. SEM (BSE) image, specimen no. CMR-5052.

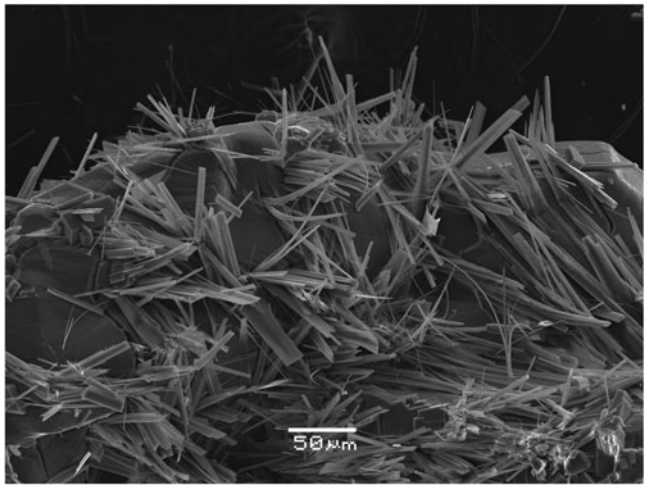

Fig. 4. Abundant lath-shaped to acicular crystals of antofagastaite on massive syngenite crystals. Arsenatnaya fumarole, Tolbachik volcano. SEM (SE) image, specimen no. Tolb-6225.

Physical properties and optical data

Antofagastaite is transparent and colourless with a white streak. It has a vitreous lustre and does not fluoresce under ultraviolet light. It is brittle, the Mohs' hardness is *ca* 3. There are two directions of distinct cleavage observed under the microscope, one of which is definitely (001); the fracture is uneven. Density measured by flotation in heavy liquids (bromoform + hexane) is 2.42(1) g cm^{-3}. Density calculated using the empirical formula is 2.465 g cm^{-3}. Some lower values of the measured density in comparison with the calculated one is caused by a slight porosity, observable in the crystals (Fig. 3).

Antofagastaite is optically biaxial (–), $\alpha = 1.489(2)$, $\beta = 1.508(2)$, $\gamma = 1.510(2)$ (589 nm), $2V_{meas.} = 40(10)°$ and $2V_{calc.} = 36°$. Dispersion of optical axes is strong with $r > v$. Optical orientation is $Z = a$. Under the microscope the crystals are colourless and nonpleochroic.

Infrared spectroscopy

In order to obtain an infrared (IR) absorption spectrum of antofagastaite (holotype: Fig. 5), the powdered sample of the mineral was mixed with dried KBr, pelletised, and analysed using an ALPHA FTIR spectrometer (Bruker Optics) with a resolution of 4 cm^{-1} and 16 scans. The IR spectrum of an analogous pellet of pure KBr was used as a reference.

Wavenumbers of absorption bands in the IR spectrum of antofagastaite and their assignments (cm^{-1}; s – strong band, w – weak band, sh – shoulder) are: 3598 (O–H-stretching vibrations of water molecules, a weak Hbond), 3373 and 3300sh (O–H-stretching vibrations of water molecules, medium-strengths Hbonds) 1685w, 1629w (bending vibrations of water molecules), 1220, 1153s, 1128s, 1090s and 1060sh [$\nu_3(F_2)$ – asymmetric stretching vibrations of SO_4^{2-} anions], 1015sh and 982 [$\nu_1(A_1)$ – symmetric stretching vibrations of SO_4^{2-} anions), 758 (librational vibrations of water molecules: see Gerakines *et al.*, 1995), 656 and 613 [$\nu_4(F_2)$ – bending vibrations of SO_4^{2-} anions], 480 and 458 [$\nu_2(E)$ bending mode of SO_4^{2-} anions]. Very weak absorptions

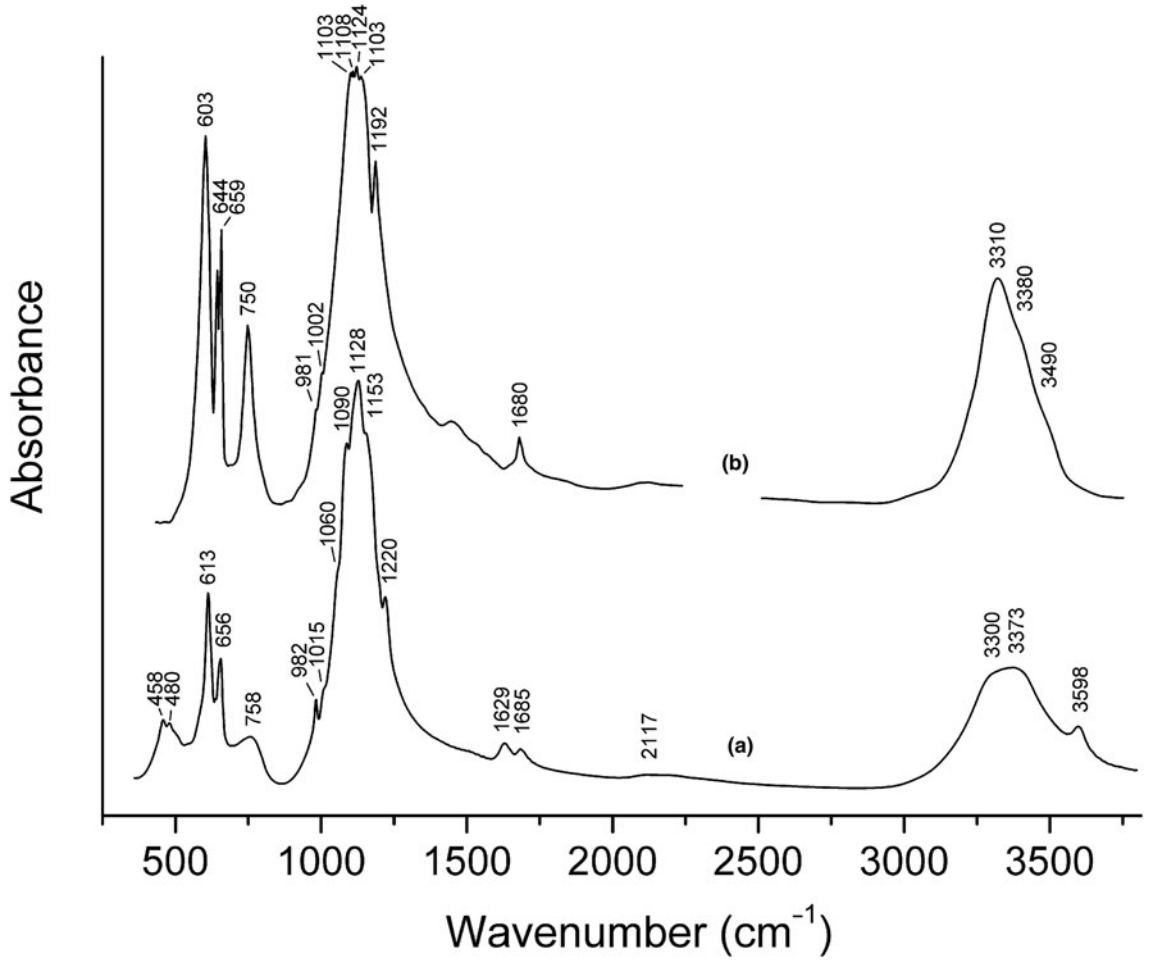

Fig. 5. Powder infrared absorption spectra of (*a*) antofagastaite from the Coronel Manuel Rodríguez mine and (*b*) syngenite from Kalush, Precarpathian region, Ukraine [drawn using data from (Chukanov, 2014)]. The weak band at ~1420 cm^{-1} in the IR spectrum of syngenite corresponds to an admixed carbonate.

in the range 2100–2250 cm^{-1} correspond to first overtones and combination modes of the SO_4^{2-} stretching modes.

Two bands of nondegenerate modes of H_2O molecules observed at 1685 and 1629 cm^{-1} indicate the presence of two kinds of significantly non-equivalent water molecules. The ν_1 symmetric stretching mode is inactive in the IR spectrum of MO_4 groups having the configuration of a regular tetrahedron, and the corresponding band intensity increases with the increase of distortion degree. Consequently, the strongest band in the range of symmetric stretching vibrations of SO_4^{2-} anions (i.e. in the range 960–1025 cm^{-1}) observed at 982 cm^{-1} is to be assigned to the most distorted S2B-centred tetrahedron $S2BO_4$ (see Table 4). Bands of stretching vibrations of BO_3^{3-}, CO_3^{2-} and NO_3^- anions (in the range from 1250 to 1550 cm^{-1}) are not observed.

The following empirical correlations between O–H stretching frequencies in IR spectra of minerals and O···O and H···O distances (from structural data) were established by Libowitzky (1999):

$$\nu(\mathrm{cm}^{-1}) = 3592 - 304 \cdot \times 10^9 \cdot \exp[-d(O\cdots O)/0.1321] \quad (1)$$

$$\nu(\mathrm{cm}^{-1}) = 3632 - 1.79 \cdot \times 10^6 \cdot \exp[-d(\mathrm{H}\cdots \mathrm{O})/0.2146] \quad (2)$$

It should be noted that at high frequencies (above 3500 cm^{-1}) substantial deviations from the correlations (1) and (2) are possible because O–H stretching frequencies depend not only on O···O and H···O distances, but also on the nature of cations coordinating O–H groups and H_2O molecules, as well as on the angle O–H···O, and the influence of these factors becomes most evident in the case of weak hydrogen bonds. The equations 1 and 2 predict that maximum possible values of O–H stretching frequencies for minerals are 3592 and 3632 cm^{-1}, respectively. However, e.g. for magnesium serpentines, brucite and kaolinite observed frequencies are close to 3700 cm^{-1}.

According to the correlation (1), the band at 3598 cm^{-1} in the IR spectrum of antofagastaite formally corresponds to the absence of hydrogen bond: $d(O\cdots O) = \infty$. According to the correlation (2),

Table 1. Chemical data for antofagastaite.

	Coronel Manuel Rodríguez mine (holotype)			Tolbachik volcano	Probe standard
Constituent	wt.%	Range	S.D.	wt.%	
Na_2O	20.85*	19.53–21.77	0.87	20.74	albite
CaO	17.42*	16.68–18.71	0.88	18.21	diopside
SO_3	52.56*	52.05–53.24	0.43	52.87	ZnS
H_2O	7.93			8.18**	
Total	98.76			100.00	

*Averaged for eight spot analyses; **calculated by total difference; S.D. – standard deviation.

Table 2. Powder X-ray diffraction data (d in Å) of the holotype specimen of antofagastaite.

I_{meas}	I_{calc}	d_{meas}	d_{calc}	$h\ k\ l$
100	**100**	**9.17**	**9.164**	**0 0 1**
18	9	6.25	6.252	1 0 0
8	9	5.909	5.902	$\bar{1}$ 0 1
57	**48**	**5.501**	**5.497**	**0 1 1**
9	1	4.682	4.648	1 0 1
24	25	4.636	4.624	1 1 0
32	**20**	**4.595**	**4.582**	**0 0 2**
29	31	4.480	4.477	$\bar{1}$ 1 1
7	1	4.256	4.239	$\bar{1}$ 0 2
30	**30**	**3.853**	**3.850**	**1 1 1**
14	11	3.815	3.812	0 1 2
4	4	3.613	3.608	$\bar{1}$ 1 2
59	**63**	**3.437**	**3.435**	**0 2 0**
17	12, 9	3.219	3.217, 3.216	0 2 1, $\bar{2}$ 0 1
31	**23**	**3.130**	**3.126**	**2 0 0**
43	**2, 48**	**3.058**	**3.067, 3.055**	**$\bar{1}$ 0 3, 0 0 3**
4	2	3.010	2.988	1 1 2
7	8	2.952	2.951	$\bar{2}$ 0 2
50	**77**	**2.918**	**2.913**	**$\bar{2}$ 1 1**
15	25	2.853	2.845	2 1 0
35	**3, 41**	**2.795**	**2.800, 2.791**	**$\bar{1}$ 1 3, 0 1 3**
50	**23, 5, 62**	**2.753**	**2.763, 2.754, 2.749**	**1 2 1, 2 0 1, 2 0 1**
3	9	2.712	2.712	$\bar{2}$ 1 2
14	15	2.678	2.669	$\bar{1}$ 2 2
1	1	2.565	2.556	2 1 1
18	19	2.527	2.525	$\bar{2}$ 0 3
3	2, 6	2.383	2.387, 2.370	1 2 2, $\bar{2}$ 1 3
6	2, 3	2.352	2.355, 2.351	1 1 3, $\bar{1}$ 0 4
3	3	2.328	2.324	2 0 2
12	4, 12, 3	2.289	2.291, 2.287, 2.283	0 0 4, $\bar{1}$ 2 3, 0 2 3
6	8	2.225	2.224	$\bar{1}$ 1 4
4	4	2.204	2.202	2 1 2
6	8	2.175	2.173	1 4
11	11, 2, 4	2.154	2.153, 2.150, 2.149	$\bar{3}$ 0 1, 1 3 0, 2 2 1
3	1	2.130	2.135	$\bar{1}$ 3 1
1	0.5	2.105	2.107	$\bar{3}$ 0 2
2	4	2.057	2.054	$\bar{3}$ 1 1
4	3	2.037	2.035	$\bar{2}$ 2 3
5	4	2.020	2.025	$\bar{2}$ 1 4
5	7, 2	2.014	2.015, 2.015	$\bar{1}$ 3 2, $\bar{3}$ 1 2
2	2	1.999	1.994	3 1 0
8	9	1.956	1.953	2 0 3
10	11, 20	1.928	1.940, 1.925	$\bar{1}$ 2 4, 2 2 2
3	5	1.885	1.885	1 3 2
5	12	1.866	1.865	$\bar{2}$ 3 1
4	11	1.845	1.847	2 3 0
5	9	1.834	1.832	0 3 3
3	8	1.811	1.809	$\bar{2}$ 3 2
3	2, 9	1.763	1.771, 1.761	0 1 5, 2 3 1
2	3	1.742	1.739	3 0 2
10	4, 20	1.719	1.724, 1.718	$\bar{3}$ 1 4, 0 4 0
4	7, 7	1.700	1.698, 1.696	2 2 3, $\bar{2}$ 3 3
2	1	1.693	1.691	1 3 3
5	7	1.661	1.659	2 0 4
2	3	1.633	1.631	2 3 2
4	8	1.618	1.617	2 5
1	1, 3	1.588	1.589, 1.581	$\bar{3}$ 0 5, $\bar{3}$ 2 4
1	3	1.552	1.549	$\bar{3}$ 1 5
3	2	1.543	1.538	$\bar{1}$ 1 6
1	1	1.529	1.527	0 0 6
1	2, 2	1.520	1.521, 1.515	$\bar{4}$ 1 3, $\bar{2}$ 4 1
3	2, 2, 3, 2	1.495	1.498, 1.497, 1.496, 1.491	$\bar{1}$ 4 3, 0 4 3, $\bar{2}$ 1 6, 0 1 6
1	1	1.477	1.476	$\bar{4}$ 0 4
1	1, 1, 3	1.457	1.459, 1.457, 1.456	$\bar{1}$ 3 5, $\bar{4}$ 2 1, $\bar{4}$ 2 2
2	1, 4	1.447	1.447, 1.442	4 1 1, $\bar{3}$ 2 5
2	1	1.435	1.434	$\bar{1}$ 2 6
2	3, 3	1.417	1.420, 1.417	$\bar{4}$ 2 3, 1 4 3
2	2, 1	1.404	1.404, 1.400	1 0 6, $\bar{2}$ 2 6
2	1, 1	1.383	1.385, 1.381	3 3 2, 2 4 2

(*Continued*)

Table 2. (*Continued.*)

I_{meas}	I_{calc}	d_{meas}	d_{calc}	$h\ k\ l$
1	1	1.360	1.359	4 2 1
2	3, 3, 2	1.352	1.356, 1.351, 1.350	$\bar{4}$ 2 4, $\bar{1}$ 0 7, 4 1 2
1	1, 1	1.337	1.338, 1.334	$\bar{1}$ 5 1, $\bar{2}$ 4 4
2	3, 3	1.325	1.326, 1.321	$\bar{1}$ 1 7, 2 2 5

* For the calculated pattern, only reflections with intensities ≥ 0.5 are given; ** for the unit-cell parameters calculated from single-crystal data.
The strongest lines are given in bold.

the band at 3598 cm^{-1} should be assigned to a very weak hydrogen bond: d(H···O) = 2.333 Å. Consequently, the peak at 3598 cm^{-1} nearly conforms to the overlapping bands which correspond to the hydrogen bonds with the OW2···O1 and OW2–OW1 distances of 3.16 and 3.09 Å, respectively (see description of the crystal structure below). The absorption maximum at 3373 cm^{-1} and the shoulder at 3300 cm^{-1} correspond to d (O···O) distances of 2.78 and 2.74 Å, respectively, which is close to the OW1···O4 distance of 2.773 Å. Consequently, these bands can be assigned to symmetric and antisymmetric vibrations of $OW1H_2$ molecules.

The IR spectrum of antofagastaite shows a remote resemblance to that of the related mineral syngenite (curve (*b*) in Fig. 5). The absence of the band at ~3600 cm^{-1} (corresponding to weak hydrogen bands) in the IR spectrum of syngenite indicates the absence of additional H_2O molecules like those occurring at the site OW2 in the structure of antofagastaite. The singlet of bending vibrations of water molecules observed at 1680 cm^{-1} in the spectrum of syngenite is in agreement with the presence of a single site of H_2O in this K–Ca sulfate. Consequently, the additional (as compared to syngenite) bands at 1629 and 3598 cm^{-1} can be used for the evaluation of the occupancy of the OW2 site in antofagastaite.

Table 3. Crystallographic data, data collection information and structure refinement details for antofagastaite $Na_2Ca(SO_4)_2{\cdot}1.5H_2O$.

Crystal data	
Formula weight	608.39
Crystal system	Monoclinic
Space group	$P2_1/m$
Unit-cell dimensions:	
a, b, c (Å)	6.4596(4), 6.8703(5), 9.4685(7)
β (°)	104.580(4)
V, Å^3	406.67(5)
Z	2
Absorption coef. (mm^{-1})	1.42
Crystal size (mm^3)	0.24 × 0.07 × 0.06
Data collection	
Temperature (K)	296
Radiation, wavelength (Å)	Mo$K\alpha$, 0.71073
F(000)	304
θ range (°)	2.2–29.0
h, k, l ranges	$-8 \le h \le 8$, $-9 \le k \le 9$, $-12 \le l \le 12$
Total refl. collected	7865
Unique reflections (R_{int})	1143 (0.085)
Unique reflections $F > 4\sigma(F)$	793
Structure refinement	
Refinement method	Full-matrix least-squares on F^2
Weighting coef. a, b	0.0667, 1.4637
Data/restraints/parameters	1143/1/103
R_1 and wR_2 [$F > 4\sigma(F)$]	0.0571, 0.1275
R_1 and wR_2 [all data]	0.0982, 0.1442
GoF	1.04
Largest diff. peak and hole (e^- Å^{-3})	2.04, –0.71

Table 4. Fractional atomic coordinates, site occupancy factors (s.o.f.), equivalent/isotropic and anisotropic displacement parameters (U, Å^2) of atoms in antofagastaite.

	Wyck.	s.o.f.	x	y	z	U_{eq}	U^{11}	U^{22}	U^{33}	U^{12}	U^{13}	U^{23}
Na1	4*f*	1	0.1500(6)	0.0042(3)	0.8020(3)	0.0677(10)	0.143(3)	0.0183(12)	0.0267(12)	−0.0100(15)	−0.0068(15)	−0.0028(10)
Ca1	2*e*	1	0.3397(2)	0.25	0.45448(15)	0.0179(3)	0.0165(7)	0.0087(6)	0.0266(7)	0	0.0020(5)	0
S1	2*e*	1	0.8372(2)	0.25	0.49442(16)	0.0100(3)	0.0089(7)	0.0046(6)	0.0152(7)	0	0.0006(5)	0
S2A	2*e*	0.5	0.3085(7)	0.25	0.1262(4)	0.0177(8)	0.025(2)	0.0157(16)	0.0102(17)	0	0.0002(18)	0
S2B	2*e*	0.5	0.1932(7)	0.25	0.1106(4)	0.0172(8)	0.025(2)	0.0142(16)	0.0103(17)	0	0.0014(18)	0
O1	2*e*	1	0.9563(7)	0.25	0.3812(5)	0.0192(10)	0.015(2)	0.021(2)	0.021(2)	0	0.0047(18)	0
O2	2*e*	1	0.9871(7)	0.25	0.6380(5)	0.0225(10)	0.023(2)	0.019(2)	0.019(2)	0	−0.0053(19)	0
O3	4*f*	1	0.6955(4)	0.0781(4)	0.4745(3)	0.0179(7)	0.0165(15)	0.0066(14)	0.0290(17)	−0.0025(11)	0.0027(13)	0.0008(12)
O4	4*f*	1	0.2634(6)	0.0787(5)	0.2070(4)	0.0342(9)	0.061(3)	0.0197(18)	0.0241(18)	0.0119(17)	0.0151(17)	0.0088(14)
O5A	2*e*	0.5	0.1687(19)	0.25	−0.0196(11)	0.022(2)	0.034(7)	0.016(5)	0.010(5)	0	−0.005(6)	0
O5B	2*e*	0.5	0.290(2)	0.25	−0.0149(13)	0.031(3)	0.031(7)	0.045(7)	0.020(6)	0	0.011(6)	0
O6A	2*e*	0.5	0.5319(15)	0.25	0.1186(12)	0.031(2)	0.022(5)	0.035(6)	0.038(6)	0	0.012(4)	0
O6B	2*e*	0.5	−0.0329(19)	0.25	0.0614(13)	0.063(4)	0.029(7)	0.122(13)	0.031(6)	0	−0.002(5)	0
OW1	2*e*	1	0.4834(8)	0.25	0.7187(6)	0.0333(13)	0.030(3)	0.031(3)	0.034(3)	0	−0.001(2)	0
OW2	2*e*	0.5	−0.2694(17)	0.25	0.0518(11)	0.031(2)	0.037(6)	0.023(5)	0.027(5)	0	0.000(4)	0
H1	4*f*	1	0.431(9)	−0.147(8)	0.231(6)	0.046*						

*U_{iso}.

Most bands, especially those of librational and stretching vibrations of OW1, in the IR spectrum of antofagastaite (at 758 and in the range 3300–3400 cm^{-1}, respectively) are somewhat broadened compared to the similar bands of syngenite. This may be due to a disordering of the structure (including disordering of hydrogen bonds formed by OW1) due to statistical alteration of vacancies and H_2O molecules at the OW2 site.

Chemical composition

Contents of Na, Ca and S in antofagastaite were determined using a Jeol JSM-6480LV scanning electron microscope equipped with an INCA-Wave 500 wavelength-dispersive spectrometer (Laboratory of Analytical Techniques of High Spatial Resolution, Department of Petrology, Moscow State University), with an acceleration voltage of 20 kV, a beam current of 20 nA, and a beam diameter of 3 μm. Contents of other elements with atomic numbers higher than oxygen are below detection limits. For the holotype, H_2O was determined by gas chromatography of products of the mineral ignition at 1200°C with a Vario Micro cube analyser (Elementar GmbH, Germany). Analytical data are given in Table 1. The absence of B, C and N in detectable amounts is confirmed by both crystal structure and IR spectroscopy data.

The empirical formulae of two samples of the new mineral (based on 8 O atoms belonging to sulfate anions per formula unit (pfu), with all H belonging to H_2O molecules – see structure data below) are: $Na_{2.06}Ca_{0.95}S_{2.01}O_8 \cdot 1.35H_2O$ for the holotype and $Na_{2.03}Ca_{0.98}S_{2.00}O_8 \cdot 1.38H_2O$ for the specimen from Tolbachik. The simplified formula is $Na_2Ca(SO_4)_2 \cdot 1.5H_2O$, which requires Na_2O 20.31, CaO 18.37, SO_3 52.46, H_2O 8.86, total 100.00 wt.%.

X-ray crystallography

Powder X-ray diffraction data of antofagastaite (Table 2) were collected with a Rigaku R-AXIS Rapid II single-crystal diffractometer equipped with a cylindrical image plate detector (radius 127.4 mm) using Debye-Scherrer geometry, Co$K\alpha$ radiation (rotating anode with VariMAX microfocus optics), 40 kV,

Table 5. Selected interatomic distances (in Å) and bond-valence sums (BVS, in vu) in the structure of antofagastaite. Distances not considered as bonds are given in italics.

Atoms	Distance	BVS	Atoms	Distance	BVS	Atoms	Distance
Na1–OW2	2.242(7)	0.153(3)*	S1–O2	1.457(5)	1.570(18)	OW1–H1	0.91(4) ×2
Na1–O2	2.355(4)	0.225(2)	S1–O1	1.468(5)	1.523(22)	OW1–O4	2.773(5)
Na1–O5A	2.370(8)	0.108(2)*	S1–O3	1.477(3) ×2	1.488(11)		
Na1–O6B	2.406(9)	0.098(3)*	<S1–O>	1.470	Σ = 6.071	OW2–O6B	1.51(2)
Na1–O5B	2.426(9)	0.093(2)*				OW2–O6A	1.57(2)
Na1–O1	2.435(4)	0.181(2)	S2A–O5A	1.447(11)	1.614(19)	OW2–OW1	3.09(2)
Na1–O6A	2.657(8)	0.050(1)*	S2A–O6A	1.463(10)	1.545(21)	OW2–O1	3.16(2)
Na1–O4	2.711(5)	0.086(1)	S2A–O4	1.472(4) ×2	1.508(18)		
Na1–OW1	2.994(6)	0.040(1)	<S2A–O>	1.464	Σ = 6.175		
Na1–O3	*3.079(4)*	*0.032(1)*					
<Na1–O>	2.551	Σ = 1.033	S2B–O6B	1.417(13)	1.750(23)		
			S2B–O5B	1.475(12)	1.496(18)		
Ca1–O3	2.380(3) ×2	0.328(3)	S2B–O4	1.488(4) ×2	1.444(17)		
Ca1–O1	2.398(4)	0.312(4)	<S2B–O>	1.467	Σ = 6.134		
Ca1–OW1	2.440(5)	0.279(4)					
Ca1–O3	2.549(3) ×2	0.208(2)	S2A–S2B	0.722(4)			
Ca1–O4	2.555(3) ×2	0.204(2)					
<Ca1–O>	2.476	Σ = 2.069					

* BVS values divided by two, according to site occupancy factors (= 0.5) of the O5A/B, O6A/B and OW2 sites.

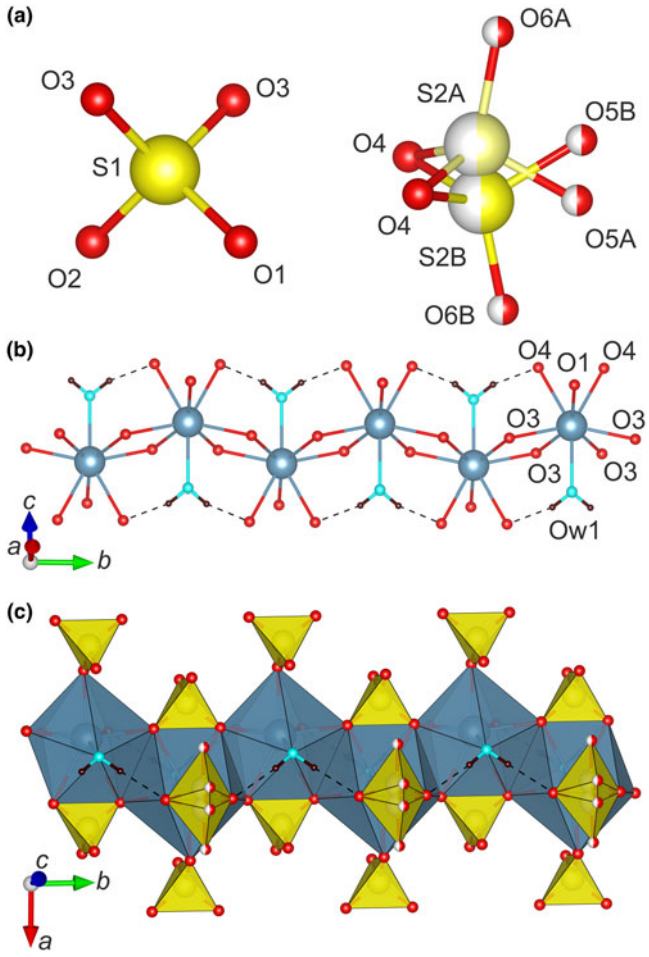

Fig. 6. Coordination of S^{6+} in the crystal structure of antofagastaite (*a*). Ball-and-stick and polyhedral representations of the chains formed by $CaO_7(H_2O)$ polyhedra are shown in (*b*) and (*c*), respectively. Ordered $S1O_4$ and disordered $S2O_4$ tetrahedra (yellow) are added in (*c*). One-half occupied sites are shown by striped balls.

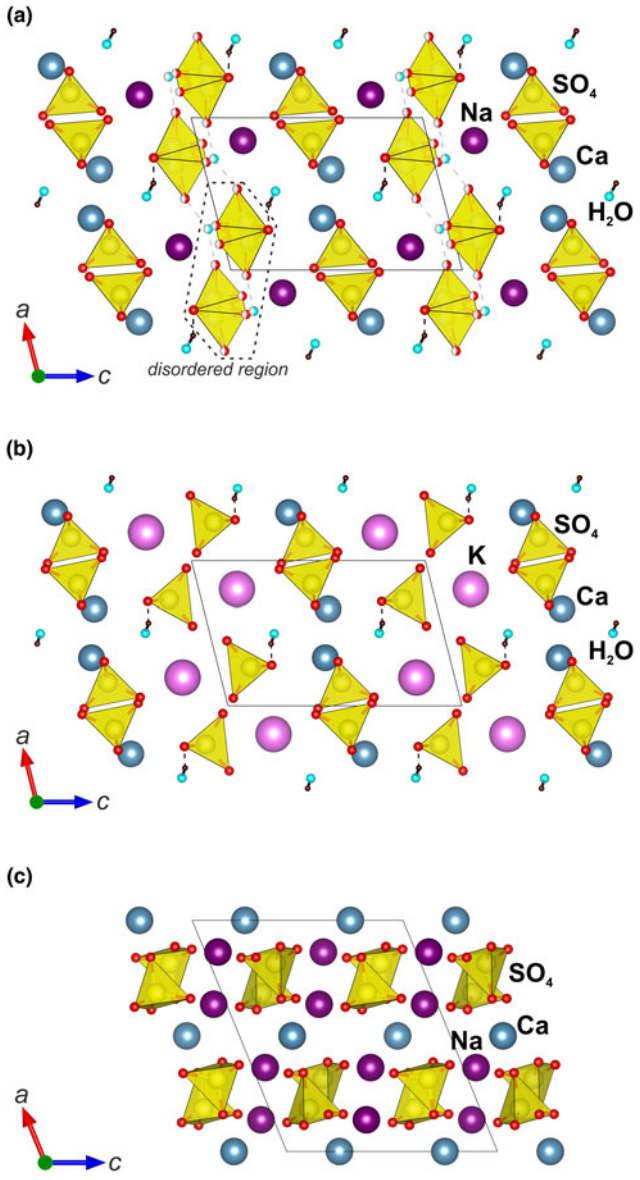

Fig. 7. Crystal structures of (*a*) antofagastaite $Na_2Ca(SO_4)_2{\cdot}1.5H_2O$; (*b*) syngenite $K_2Ca(SO_4)_2{\cdot}H_2O$; and (*c*) glauberite $Na_2Ca(SO_4)_2$ projected along the *b* axis. One-half occupied sites are shown by stripped balls in antofagastaite. The unit cells are outlined.

15 mA and exposure 15 min. Angular resolution of the detector is 0.045° in 2θ units (pixel size is 0.1 mm). The data were integrated using the software package *Osc2Tab* (Britvin *et al.*, 2017). Unit-cell parameters refined from the powder data for the holotype specimen are as follows: $a = 6.463(3)$, $b = 6.867(2)$, $c = 9.467(4)$ Å, $\beta = 104.47(4)°$ and $V = 406.8(4)$ Å^3.

Single-crystal X-ray diffraction studies were carried out using a Bruker D8 Venture diffractometer with a micro-focus X-ray tube operated with Mo*K*α radiation (λ = 0.71073 Å) at 50 kV and 1 mA. More than a half of the Ewald sphere was collected with frame widths of 0.5° in *ω*, and a 50 s count time for each frame.

The diffraction data were integrated and corrected for absorption using a multi-scan type model using the *APEX* and *SADABS* Bruker programs. The unit-cell parameters of antofagastaite [$a = 6.4596(4)$, $b = 6.8703(5)$, $c = 9.4685(7)$ Å, $\beta = 104.580(4)°$, $V = 406.67(5)$ Å^{3}and $Z = 2$ in $P2_1/m$] were determined and refined by least-squares techniques on the basis of 2751 reflections. The crystal structure of antofagastaite was solved in space group $P2_1/m$ by the charge-flipping method, using the *SUPERFLIP* program (Palatinus and Chapuis, 2007) and refined to $R_1 = 0.057$ by means of the *SHELX* program (Sheldrick, 2015). All atoms sites were refined anisotropically. Positions of hydrogen atoms of the fully occupied water OW1 site were taken from the difference-Fourier maps. Hydrogen positions of the one-half occupied water OW2 site were not determined. The main crystallographic information is summarised in Table 3.

One relatively large residual electron density peak (2.04 e$^-$ Å^{-3}) was observed in the difference-Fourier maps on the final stages of refinement. However, its attribution to an additional O position of a water molecule or to metal cations in the structure of antofagastaite remains ambiguous due to its very low occupancy as refined. Fractional atomic coordinates, thermal displacement parameters, selected interatomic distances, and bond-valence sums for the structure of antofagastaite are listed in Tables 4–5. The crystallographic information file has been deposited with the Principal Editor of *Mineralogical Magazine* and is available as Supplementary material (see below).

One small (0.03 mm × 0.03 mm × 0.1 mm) prismatic crystal of antofagastaite from the Arsenatnaya fumarole, Tolbachik volcano, was also studied by the means of single-crystal X-ray diffraction. The obtained space group $P2_1/m$ is the same and unit-cell

Table 6. Comparative data for antofagastaite and syngenite.

	Antofagastaite*	Syngenite
Formula	$Na_2Ca(SO_4)_2 \cdot 1.5H_2O$	$K_2Ca(SO_4)_2 \cdot H_2O$
Crystal system	Monoclinic	Monoclinic
Space group	$P2_1/m$	$P2_1/m$
a (Å)	6.4596(4)	6.225(2)
b (Å)	6.8703(5)	7.127(2)
c (Å)	9.4685(7)	9.727(3)
β (°)	104.580(4)	104.153(25)
V (Å^3)	406.67(5)	418.4(3)
Z	2	2
Powder XRD data		
Strongest reflections of the powder XRD pattern: *d* (Å) – *I*	9.17–100 5.501–57 4.595–32 3.437–59 3.130–31 3.058–43 2.918–50 2.795–35 2.753–50	9.49–40 5.71–55 4.624–40 3.165–75 2.855–100 2.827–50 2.741–55
Optical data		
α	1.489	1.501
β	1.508	1.517
γ	1.510	1.518
Optical sign, 2V	(–), 40°	(–), 28°
References	This work	Bokiy *et al.* (1978); Anthony *et al.* (2003)

*Data for the holotype are given.

parameters [$a = 6.427(6)$, $b = 6.785(8)$, $c = 9.44(1)$ Å, $\beta = 105.03(2)°$ and $V = 397.6(8)$ Å^3] are nearly identical to those of the holotype specimen of antofagastaite from the Coronel Manuel Rodríguez mine described above. The crystal structure of anthofagastaite from Tolbachik was solved ($R_1 = 7.1\%$) and proved to be identical to that of the holotype, including the disorder of one of the sulfate groups and H_2O molecules.

Crystal structure: description and discussion

There are two symmetrically independent S sites (Fig. 6*a*) in antofagastaite. The S1 site is ordered and demonstrates a regular tetrahedral coordination environment (<S1–O> = 1.470 Å, 6.07 valence units, vu), whereas the S2 site is split over S2A (<S2A–O> = 1.464 Å, 6.18 vu) and S2B (<S2B–O> = 1.467 Å, 6.13 vu) sites with s.o.f. of 0.5 per each. There is a positional disorder also observed for O5 and O6 sites coordinating atom S2.

One symmetrically independent Ca site is coordinated by seven oxygen atoms and one water molecule (Fig. 6*b*). Ca–O distances lie in the range of 2.380–2.555 Å (2.07 vu). $CaO_7(H_2O)$ polyhedra share common edges, thus, forming the chains depicted in Fig. 6*b*. Sulfate tetrahedra decorate Ca-centred chains in bidentate and monodentate fashions (Fig. 6*c*).

The Na site coordination environment is irregular due to the presence of disordered O5 and O6 sites and partially occupied water molecules. Na–O bond lengths vary from 2.242 Å to 2.994 Å.

The structure of antofagastaite consists of ordered and disordered blocks (Fig. 7*a*). Generally, the structure is similar to that described previously for syngenite $K_2Ca(SO_4)_2 \cdot H_2O$ (Corazza and Sabelli, 1967; Bokiy *et al.*, 1978; Ballirano *et al.*, 2005) (Fig. 7). Antofagastaite and syngenite also demonstrate a close relationship in symmetry, unit-cell parameters, powder X-ray patterns and optical characteristics (Table 6). However, no solid solution between these minerals is observed. The difference between antofagastaite and syngenite is clearly demonstrated by the paragenetic association of them found in the Arsenatnaya fumarole (Fig. 4) in which both minerals are chemically very close to the end-members.

The crystal structure of syngenite (Fig. 7*b*) is characterised by a lower content of water molecules. Intrusion of additional water molecules in the syngenite structure type results in disorder of the one of the two tetrahedral sulfate groups (Fig. 8) observed in antofagastaite (Fig. 7*a*). Hence, the split into two half-occupied conformations results in a row of sulfate tetrahedra oriented towards each other by their apices along [100] with a water molecule located between them with a 50% probability.

Note also that the antofagastaite crystal structure is significantly different from the chemically closely related but anhydrous mineral glauberite $Na_2Ca(SO_4)_2$ (Araki and Zoltai, 1967) (Fig. 7*c*).

The crystal structure of antofagastaite contains 1.5 H_2O molecules pfu, which are located in one fully occupied OW1 site and in

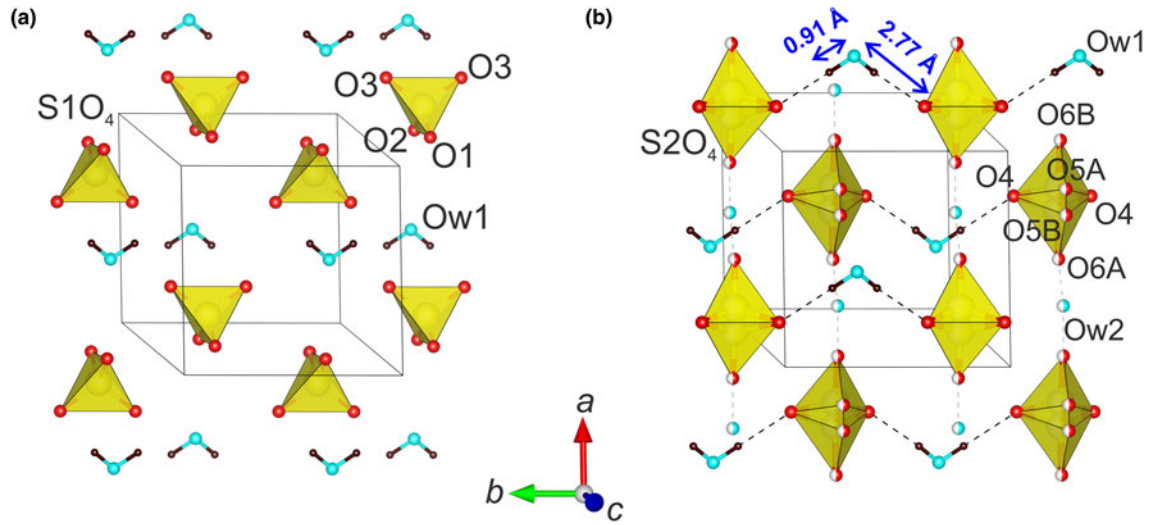

Fig. 8. General projection of the arrangement of the (*a*) ordered $S1O_4$ tetrahedra and OW1 water molecules and (*b*) disordered $S2O_4$ tetrahedra with OW1 and OW2 water molecules in the crystal structure of antofagastaite. One-half occupied sites are shown by striped balls.

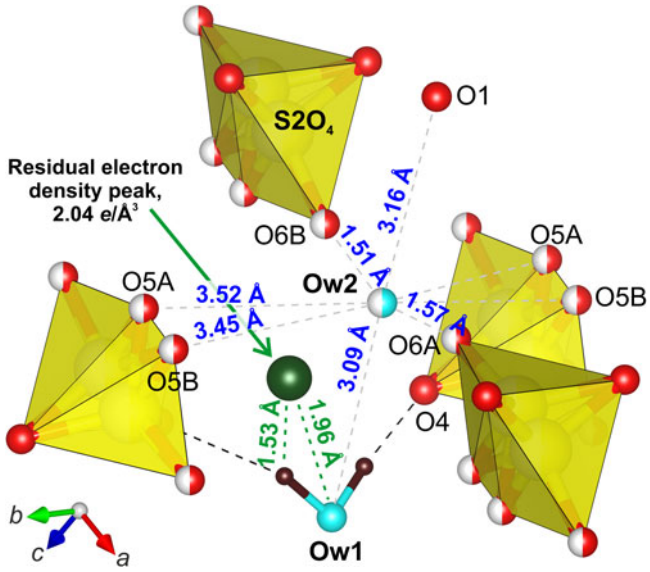

Fig. 9. Atomic situation surrounding the OW2 site in the crystal structure of antofagastaite. The highest maximum of the residual electron density localised from the difference-Fourier map is represented by a dark green ball. One-half occupied sites are shown by striped balls.

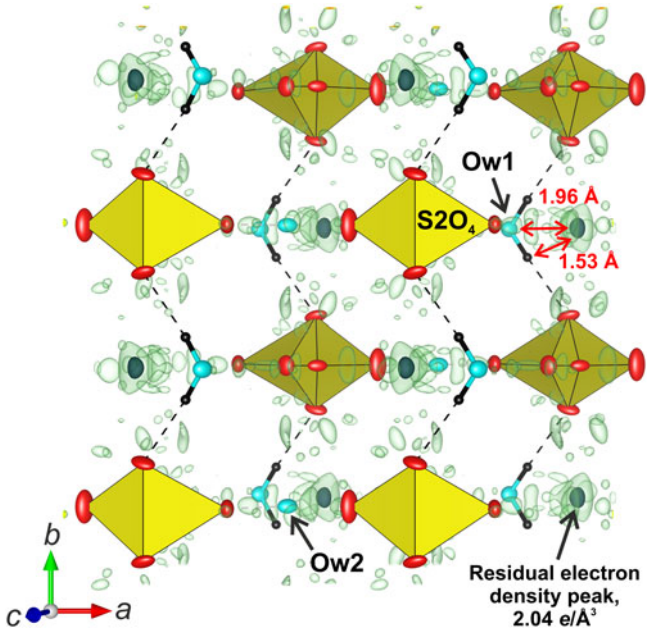

Fig. 10. Fragment of the antofagastaite structure and isosurfaces corresponding to the maxima of the difference-Fourier electron density shown with a boundary condition of 0.7 e^- Å^{-3} (light green). The highest maximum is localised and displayed by a black spot (boundary condition of 2.0 e^- Å^{-3}). Displacement ellipsoids are drawn at the 50% probability level.

one half-occupied OW2 site. Hydrogen atoms of the OW1 molecule localised from the difference-Fourier electron density map result in OW1–H1 and H1···O4 distances of 0.95(4) Å and 1.87(5) Å, respectively (Fig. 8*b*). A similar atomic surrounding of the one symmetrically independent water molecule was reported in the syngenite structure: OW–H = 0.82(5) Å and H···O = 1.90(5) Å (Bokiy *et al.*, 1978).

The presence of a 0.5 vacancy and the occurrence of several possible H-bond acceptor-anions shown in Fig. 9 make the localisation of hydrogen atoms of the half-occupied OW2 water molecule impossible.

We note the presence of the maximum positive difference-Fourier peak of 2.04 e^- Å^{-3} located at the distances of only 1.96 Å from the OW1 site and of 1.53 Å from its hydrogen atoms (Fig. 9). Attribution of this peak to an O atom of an additional water molecule may provide 0.12 additional H_2O. However, we believe that the structure of antofagastaite contains exactly 1.5 H_2O, which is constrained to this amount as a function of the neighbouring disordered $S2O_4$ tetrahedra, and, thus, the peak cannot be assigned to a water molecule. As shown in Fig. 10, the residual peak is comparable with the overall noise level within the difference-Fourier map and, thus, it may be ignored in the final structure model of antofagastaite.

Acknowledgements. We thank Gerald Giester, Peter Leverett, František Laufek and anonymous referee for valuable comments. This study was supported by the Russian Science Foundation, grant no. 16-17-10085 (X-ray diffraction and structural studies). The technical support by the SPbSU X-Ray Diffraction Resource Center is acknowledged.

Supplementary material. To view supplementary material for this article, please visit https://doi.org/10.1180/mgm.2019.17.

References

Anthony J.W., Bideaux R.A., Bladh K.W. and Nichols M.C. (2003) *Handbook of Mineralogy, Volume: V. Borates, Carbonates, Sulfates*. Mineral Data Publishing, Tucson, 813 pp.

Araki T. and Zoltai T. (1967) Refinement of the crystal structure of a glauberite. *American Mineralogist*, **52**, 1272–1277.

Ballirano P., Belardi G. and Maras A. (2005) Refinement of the structure of synthetic syngenite $K_2Ca(SO_4)_2{\cdot}H_2O$ from X-ray powder diffraction data. *Neues Jahrbuch für Mineralogie - Abhandlungen*, **182**, 15–21.

Bokiy G.B., Pal'chik N.A. and Antipin M.Y. (1978) More precise determination of syngenite crystal structure. *Kristallografiya*, **23**, 257–260 [in Russian].

Britvin S.N., Dolivo-Dobrovolsky D.V. and Krzhizhanovskaya M.G. (2017) Software for processing the X-ray powder diffraction data obtained from the curved image plate detector of Rigaku RAXIS Rapid II diffractometer. *Zapiski Rossiiskogo Mineralogicheskogo Obshchestva*, **146**, 104–107 [in Russian].

Chukanov N.V. (2014) *Infrared Spectra of Mineral Species: Extended Library*. Springer Verlag, Dordrecht, 1716 pp.

Corazza E. and Sabelli C. (1967) The crystal structure of syngenite, $K_2Ca(SO_4)_2{\cdot}H_2O$. *Zeitschrift für Kristallographie*, **124**, 398–408.

Freyer D., Reck G., Bremer M. and Voigt W. (1999) Thermal behaviour and crystal structure of sodium-containing hemihydrates of calcium sulfate. *Monatshefte für Chemie*, **130**, 1179–1193.

Gerakines P.A., Schutte W.A., Greenberg J.M. and van Dishoeck E.F. (1995) The infrared band strengths of H_2O, CO and CO_2 in laboratory simulations of astrophysical ice mixtures. *Astronomy and Astrophysics*, **296**, 810–818.

Leverett P. and Williams P.A. (2007) Unusual post-mining sulfates from the Peelwood and Lloyd mines, New South Wales, and a comment on wattevilleite. *Australian Journal of Mineralogy*, **13**, 41–46.

Libowitzky E. (1999) Correlation of O–H stretching frequencies and O–H···O hydrogen bond lengths in minerals. *Monatshefte für Chemie*, **130**, 1047–1059.

Mees F., Hatert F. and Rowe R. (2008) Omongwaite, $Na_2Ca_5(SO_4)_6{\cdot}3H_2O$, a new mineral from recent salt lake deposits, Namibia. *Mineralogical Magazine*, **72**, 1307–1318.

Mills S.J., Kampf A.R., Dini M. and Molina A. (2012) Die weltbesten Destinezit-Kristalle und andere seltene Sulfate von Mejillones, Chile. *Mineralien-Welt*, **23**, 73–81. (In German).

Palache C. and Foshag W.F. (1938) Antofagastite and bandylite, two new copper minerals from Chile. *American Mineralogist*, **23**, 85–90.

Palache C., Berman H. and Frondel C. (1951) *The System of Mineralogy of James Dwight Dana and Edward Salisbury Dana Yale University 1837–1892. Volume II: Halides, Nitrates, Borates, Carbonates, Sulfates, Phosphates, Arsenates, Tungstates, Molybdates, etc.* John Wiley and Sons, Inc., New York, 7th edition, revised and enlarged, 1124 pp.

Palatinus L. and Chapuis G. (2007) SUPERFLIP – a computer program for the solution of crystal structures by charge flipping in arbitrary dimension. *Journal of Applied Crystallography*, **40**, 786–790.

Pekov I.V., Koshlyakova N.N., Zubkova N.V., Lykova I.S., Britvin S.N., Yapaskurt V.O., Agakhanov A.A., Shchipalkina N.V., Turchkova A.G. and Sidorov E.G. (2018) Fumarolic arsenates – a special type of arsenic mineralization. *European Journal of Mineralogy*, **30**, 305–322.

Pekov I.V., Lykova I.S., Agakhanov A.A., Belakovskiy D.I., Vigasina M.F., Britvin S.N., Turchkova A.G., Sidorov E.G. and Scheidl K.S. (2019) New arsenate minerals from the Arsenatnaya fumarole, Tolbachik volcano, Kamchatka, Russia. XII. Zubkovaite, $Ca_3Cu_3(AsO_4)_4$. *Mineralogical Magazine*, **83**, https://doi.org/10.1180/mgm.2019.33

Sabelli C. and Trosti-Ferroni R. (1985) A structural classification of sulfate minerals. *Periodico di Mineralogia*, **54**, 1–46.

Sheldrick G.M. (2015) Crystal structure refinement with SHELXL. *Acta Crystallographica*, **C71**, 3–8.

Slyusareva M.N. (1969) Hydroglauberite, a new mineral of the hydrous sulfate group. *Zapiski Vsesoyuznogo Mineralogicheskogo Obshchestva*, **98**, 59–62 [in Russian].

Vergouwen L. (1981) Eugsterite, a new salt mineral. *American Mineralogist*, **66**, 632–636.